

## Chapter 3

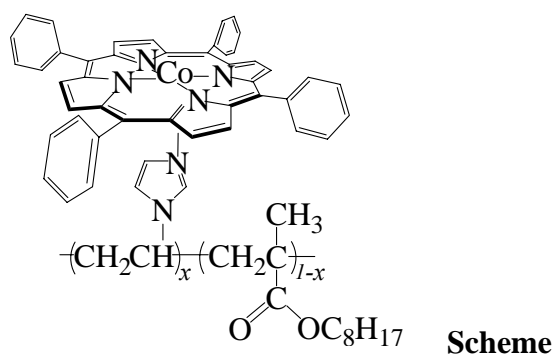
### Preparation and Structure of the Thin Membrane of Polymeric Cobaltporphyrin Complex

#### 3.1 Introduction

The separation process of mixed gases such as (oxygen/nitrogen) and (carbon dioxide/methane) using a polymer membrane due to the advantageous of simple and compact separator, convenient operation, low operating costs, etc., and has been used in actual applications.<sup>1,2</sup> For each permeation module, the polymer membrane is an asymmetric membrane which a combined sub-micron ordered solid thin membrane as an active layer with a porous support. That is, the success of the gas separation is dependent on the separation performance of the active thin layer. It is difficult to prepare a polymer in which only the oxygen solubility coefficient is substantially enhanced. However, as typified by the separation of oxygen/nitrogen, for the separation of a gas molecule, which has a similar radius and physical property, a negative correlation exists between the permeability and permselectivity through the membrane<sup>3</sup>.

It has been noted that a polymer membrane containing metal complexes specifically and reversibly interacts with gaseous molecules making it suitable for efficient gas separation.<sup>4</sup> Facilitated transport is defined as a process in which a carrier molecule forms a complex with a specific component, thereby increasing the transport rate of this component relative to other components in the feed stream. Some polymer membranes have been reported which have the ability of facilitated transport<sup>5</sup>. The authors have reported this specific and reversible oxygen-binding reaction that established a concentration gradient of oxygen across the membrane from the upstream side to the downstream side and produced the facilitated oxygen transport.<sup>5,6</sup> However, the membrane is hardened with the addition of the carrier for facilitated transport (e.g., for oxygen facilitated transport, the porphyrin complex)<sup>7</sup>. The inhibition of the physical permeation and the purpose of increasing the permselectivity combined to give a lower gas permeation compared with the permeation through the normal gas separation membrane (permeability coefficient ca.  $10^{-10}$  cm<sup>3</sup> (STP) cm/ cm<sup>2</sup> s cmHg). To increase the permeation with a high permselectivity, it is essential to make an active thin polymer membrane containing a carrier (complex).

Recently, facilitated transport membranes containing a Ag salt as a fixed olefin carrier that selectively and reversibly facilitates olefin such as propylene and ethane were reported by Dr. Kang et al.<sup>8,9</sup> The prepared membrane contained a Ag complex



such as polyvinylpyrrolidone or polyoxazoline with a high Ag salt content. A high barrier ability from the gas, large flux and high permselectivity ( $> 5000$ ) were obtained during the (propylene/propane) separation.

The present chapter describes the preparation of the oxygen permselective polymeric porphyrin membrane with a sub-micron thickness in order to maintain a high oxygen flux. As for the oxygen carrier, a simple and planar cobalt-tetraphenylporphyrin was used. Based on the selection of the support membrane, and the membrane preparation method, the polymer complex thin membrane was successfully prepared with an extremely high porphyrin (carrier) content. Since the (oxygen/nitrogen) permselectivity through this membrane was  $> 100$  while the oxygen permeability coefficient was  $10^{-9} \text{ cm}^3(\text{STP}) \text{ cm} / \text{ cm}^2 \text{ s cmHg}$ , a homogeneous distribution of the cobalt-5,10,15,20-tetraphenylporphyrin (CoTPP) throughout the membrane and complexation with the imidazolyl residue of the poly(octyl methacrylate-co-1-vinylimidazole) (OIIm) with a 5-coordinated structure are described.

## 3.2 Experimental

### 3.2.1 Material

CoTPP was purchased from Aldrich Co. and used without further purification. 1-Vinylimidazole (Tokyo Kasei, bp.  $80^\circ\text{C}/4\text{mmHg}$ ) and octyl methacrylate (Tokyo Kasei, bp  $65^\circ\text{C}/12\text{mmHg}$ ) were purified by vacuum distillation. Tetrahydrofuran(THF) was distilled prior to use.

### 3.2.2 Polymer ligand

The copolymerization procedure was as follows. 15ml (0.06mol) of vinylimidazole and 21ml (0.09mol) of octyl methacrylate were dissolved in 36ml of toluene and 24ml of ethanol, and 0.03mg (183mmol) of azobisisobutyronitrile was added. This mixture was heated at  $65^\circ\text{C}$  for 4 hr. The reaction mixture was added dropwise into a large amount of methanol. The precipitate was dissolved in chloroform and purified by reprecipitation. Yield 0.37g (37%). The molecular weight of the copolymer composition

was determined to be 30mol% by elemental analysis.

### 3.2.3 Membrane preparation

OIm (3.7mg, [Imidazolyl residue of OIm]=13mmol/l) was dissolved in tetrahydrofuran (0.5ml) and CoTPP (2.8mg, [CoTPP]=8.1mmol/l) was added to the solution under an oxygen-free atmosphere. The solution was carefully cast onto a polyacrylonitrile porous support membrane (GMT Membrantechnik, BRD) with a coating bar (R K Print Coat Instruments, Inc.) to yield the active thin CoTPP-OIm layer with a sub-micron thickness (e.g., 85 nm from SEM). The membranes were kept in a nitrogen atmosphere for ca. 3hrs and dried in vacuo overnight at room temperature.

### 3.2.4 X-ray photoelectron spectroscopy (XPS) measurement

The XPS spectra were acquired using ESCALAB 250 electron spectrometer (VG Scientific Co., Ltd.) with monochromated Al K $\alpha$  X-rays at 100W. The main chamber of the XPS instrument was maintained at  $10^{-7}$  Torr.

The sectional distribution of the CoTPP was measured by angle-resolved XPS. By assuming that the X-ray intensity does not diminish within the XPS sampling depth, the relation between the intensity,  $I_i$ , and concentration,  $X_i$ , of an element  $i$  can be described as a function of the electron escape depth. If XPS intensities of the film and substrate are measured for several takeoff angles, one photoelectron peak from the film and one from the substrate are chosen so that there is no contribution if the substrate elements affect the film peak intensity.

The sampled vertical depth, from which 95% of the XPS signal intensity originates, is  $d = 3\lambda \cos\theta$ <sup>10</sup> where  $\lambda$ , and  $\theta$  are the effective escape depth and the takeoff angle from the normal surface, respectively. Despite the polymer material, for almost all the polymer samples, the  $\lambda$  value is about 3nm<sup>11</sup>. Since the escape depth of the X-ray is about 10nm, it is possible with the relative index in the  $\cos\theta$  depth direction. In the component of the CoTPP-OIm complex, the ratio of the carbon is significant, therefore, no in-depth concentration dependency is observed.

The ratio of the cobalt to the carbon in the complex component is as small as ca. 1.0%; the distribution of the cobalt element in-depth is measured by varying the takeoff angle and calculating the ratio of the signal intensity of cobalt to that of carbon.

The XPS spectra were obtained at the eight takeoff angles (relative to the surface normal) of 0, 15, 30, 45, 50, 60, 70, and 80. The relative photoelectron intensities of the C 1s and Co 2p peaks were evaluated from the peak areas after subtraction of the liner a background.

### 3.2.5 Gas permeability measurement

The permeation properties of the composite membrane were investigated with oxygen or nitrogen at room temperature. The feed pressure was 1 or 76 cmHg (gauge pressure, the real feed pressure is 77 or 156 cmHg), while the permeate-side pressure was atmospheric. The volumetric gas flow rates were measured with a soap-bubble flowmeter. The permeability coefficients ( $P$ , 1Barrer =  $10^{-10}$  cm<sup>3</sup> (STP) cm/ cm<sup>2</sup> s cmHg) of oxygen and nitrogen were calculated by the flux which was normalized by the pressure difference between the upstream and downstream, temperature, and membrane thickness.

### 3.2.6 Other measurements

X-ray diffraction was performed using a RINT 1100 (Rigaku, Tokyo) x-ray diffractometer with Fe-K $\alpha$  radiation operating at 40kV and 80mA. Diffractograms were obtained from 5 to 50 degrees with a scanning speed of 0.6 degree per minutes. The solid CoTPP and the CoTPP-OIm membranes were used for the experiments.

The UV and IR spectra were obtained using V550 and FT/IR 420 spectrometers (JASCO) respectively. The CoTPP-OIm membranes were prepared in the same manner as described in section 2.3. The samples are placed in a high pressure cell (shown in Figure 3-1) and the transmission spectra of the membranes were obtained from 0 to 7 atm. The coordination structure of the polymer-coordinated CoTPP-OIm membrane was studied by ESR spectroscopy (JEOL RE-2X spectrometer) operating at X-band at 77K, setting the membrane piece in a glass tube with a vessel for deaeration. The magnetic

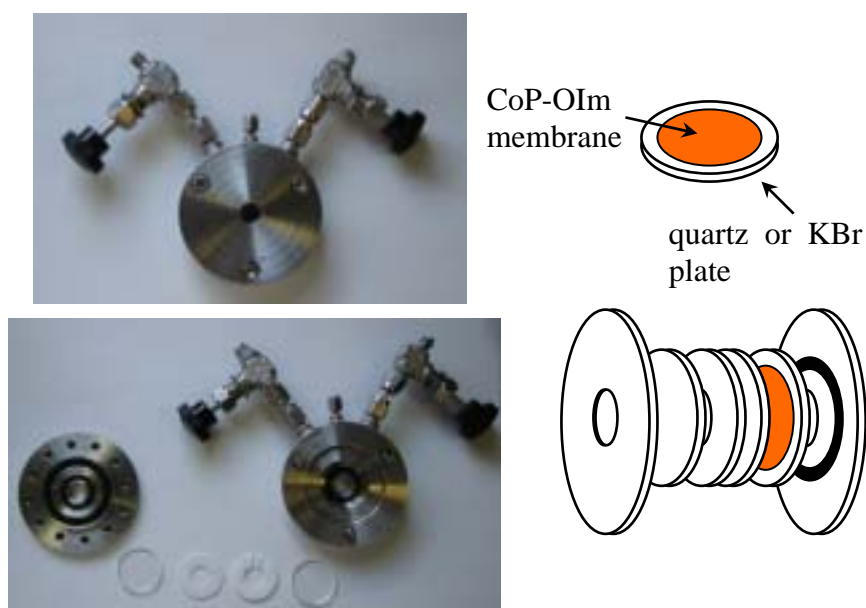


**Figure 3-1.** High pressure cell for the spectroscopic measurement.

fields were corrected with the splitting of Mn(II) in MnO.

Scanning electron micrographs were obtained using an SEM S4500S (Hitachi) at a 25kV accelerated voltage. The sample were immersed in liquid N<sub>2</sub> and cut to make a fresh section. The samples coated with Pd-Pt ions deposition were used for the measurement.

Atomic Force Microscopy, AFM, was performed using a Nanoscope III (Digital Instruments, Inc.). The AFM image of the CoTPP-OIm membrane surface was obtained in the tapping mode at a scan rate of 1 Hz. The resonance frequency of ca. 267 kHz was selected upon tuning.

The samples for the transmission electron microscopy (TEM) were prepared as follows: the membrane was cut in small pieces and was embedded in epoxy resin (Spurr resin) and cured for 8h at 70°C. The resulting samples were initially trimmed with an ultramicrotome (JEOL EM-SUPERNOVA) at room temperature using a glass trimming knife, and finally ultra-thin sectioned using a diamond knife (Sumi knife, Sumitomo Electric Ind.). The section thickness was 60nm. The ultra-thin sections were placed on a 400-mesh micro grid and studied using a JEM-100CX (JEOL) transmission electron microscope operating at 100kV. To clarify the gap of the electron density between the support membrane and active porphyrin layer more clearly, platinum *meso*-tetra(pentafluorophenyl) porphyrin was used instead of the CoTPP in the TEM measurement.

### 3.3 Membrane preparation and morphology of the CoTPP-OIm membrane

The effect of the facilitated transport is increased with the concentration of the carrier in the polymer matrix. The glass transition temperature ( $T_g$ ), however, is increased with the carrier content in the membrane, therefore, the ability of the membrane preparation decreases, (e.g., using OIm,  $T_g$  increases from -0.6 to 6 °C with an increase in the CoTPP into the membrane up to 42wt%).

Upon preparation of the CoTPP-OIm membrane, the molecular ratio of the imidazolyl residue to CoTPP, the casting solvent and the polymer concentration of the casting solvent, and the type of the support membrane were widely examined. THF was selected as the casting solvent since the OIm and CoTPP are easily dissolved and the side reaction, such as the Co(II)TPP, is automatically oxidized to Co(III)TPP, would not occur. The feed molar ratio of [CoTPP] / [imidazolyl residue of OIm] was 3/5 (CoTPP content = 42wt%) to introduce CoTPP in a large quantity and ligate the imidazolyl residue of the polymer. The polymer concentration of the casting solvent is *ca.* 1% (molarity of the imidazolyl residue = 13mmol/l). A PAN porous membrane was used as

the support membrane. The porous membrane of the copolymer of ethylene and propylene were also examined as a support membrane, but the polymer solution that penetrated into the membrane pore and the polymer became stuck after the casting solvent was evacuated. The CoTPP-OIm solution is coated using the bar coater under a nitrogen atmosphere to avoid the oxidation of Co(II)TPP. The membrane of the CoTPP-OIm complex was successfully prepared with a submicron thickness. The obtained membrane was orange, transparent, and homogeneously colored on the support membrane.

Atomic force microscopy was first used to study the surface image of the support membrane (Figure 3-2) and the CoTPP-OIm membrane coated on it. The surface image of the support membrane (Figure 3-2(a)) has a rough skin, about 15nm on the upper and lower sides, about a 60nm horizontal direction which allows that the PAN support membrane to overlap with the fine fiber. On the other hand, the surface of the CoTPP-OIm membrane has a smooth skin (Figure 3-2(b)), therefore, the CoTPP-OIm membrane should have no defects or pin holes. Studying a wide area produced similar images and the homogeneous and pinhole-less structure of the CoTPP-OIm membrane was confirmed.

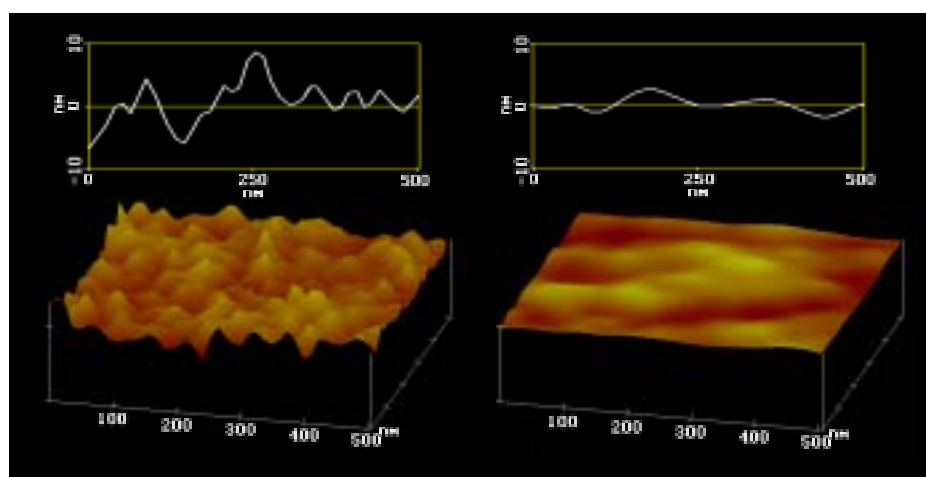


**Figure 3-2.** AFM images of the polyacrylonitrile porous supporting membrane (a) and the CoTPP-OIm membrane on the supporting membrane (b).

A sectional view of the CoTPP-OIm membrane is shown in Figure 3-3. The fibril structure of the PAN support membrane is clearly shown on the bottom side in SEM photograph. The upper end, the CoTPP-OIm film, is shown to have been created with a uniform layer. The boundary surface of the CoTPP-OIm film and the support membrane clearly appeared, and the CoTPP-OIm shouldn't not block the pores of the support membrane, and it has been formed in (support from the gas permeability coefficient of

under-mentioned) and on the supporting layer as an independent one. The CoTPP-OIm thin film was calculated to be 85nm. Everywhere on the SEM and TEM photographs the membrane showed the same thickness for the CoTPP-OIm membrane.

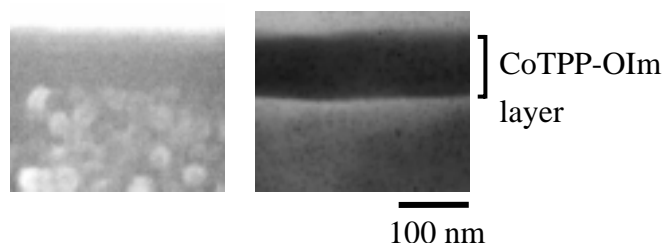


**Figure 3-3.** SEM and TEM photographs of the CoTPP-OIm membranes.

Wide angle X-ray diffraction image of this film was measured to determine the dispersion of the CoTPP in the membrane. The strongly sharp diffraction peak by the crystal appeared only in the CoTPP powder, while a wide and broad peak appeared for the OIm film and CoTPP-OIm film. This indicates that the CoTPP is uniformly dispersed as the molecule in the film in spite of such a high concentration as 40% CoTPP and that film also has an amorphous state.

The film thickness was changed by varying the concentration or the amount of the polymer complex on the support membrane. The nitrogen permeability coefficient ( $P_{N_2}$ , Table 3-1) of the CoTPP-OIm membrane is  $10^{-11} \text{ cm}^3(\text{STP}) \text{ cm} / \text{ cm}^2 \text{ s cmHg}$ , which is reasonable for the amorphous solid membrane with a  $T_g$  from 0 to room temperature.<sup>1</sup> Since  $P_{N_2}$  was constant and independent of the membrane thickness, one was able to be say that the CoTPP-OIm film was uniform and homogenous, and not immersed or stuck in the pores of the support membrane.

**Table 3-1.** Membrane thickness and nitrogen permeability coefficient ( $P_{N_2}$ ) for the CoTPP-OIm membranes at 25°C

Membrane Thickness <sup>a)</sup>	$10^{12} P_{N_2}$ <sup>b)</sup>
88	8.4
125	8.2

a) nm, b)  $\text{cm}^3(\text{STP}) \text{ cm} / \text{ cm}^2 \text{ s cmHg}$

Several upstream pressures were applied to the CoTPP-OIm membrane and the resulting permeability coefficients of the oxygen and nitrogen are listed in Table 3-2. The permeability coefficient of the nitrogen is constant and independent from the

upstream pressure and lower than that of oxygen.  $P_{O_2}$  was much larger than  $P_{N_2}$  and steeply increased with a decrease in the feed pressure. (nitrogen/oxygen) permselectivity of the CoTPP-OIm membrane at a feed pressure of 77cmHg was more than 150. These results indicate that the fixed CoTPP carrier in the membrane interacts with oxygen and facilitates oxygen transport in the membrane despite the thin membrane of under 100nm.

**Table 3-2.** Permeability coefficients of oxygen ( $P_{O_2}$ ) and nitrogen ( $P_{N_2}$ ) for the CoTPP-OIm membrane at various upstream pressures<sup>a)</sup>

Pressure (cmHg)	$10^{12} P_{O_2}$ $\frac{\text{cm}^3(\text{STP}) \text{ cm}}{\text{cm}^2 \text{ s cmHg}}$	$10^{12} P_{N_2}$ $\frac{\text{cm}^3(\text{STP}) \text{ cm}}{\text{cm}^2 \text{ s cmHg}}$	$(P_{O_2}/P_{N_2})$
77	1500	8.6	170
152	93	8.7	10

<sup>a)</sup> membrane thickness = 85nm, at 25°C.

### 3.4 Complexation of CoTPP with polymer ligand

The coordination of molecular oxygen to the Co in the CoTPP-OIm membrane was spectroscopically confirmed. The ESR spectrum of the CoTPP-OIm membrane in an oxygen-free atmosphere is shown in Figure 3-4. From the anisotropy, the CoTPP was immobilized in the OIm matrix and 8 hyperfine and triplet super hyperfine lines derived from the Co ( $I=7/2$ ) and single nitrogen nucleus ( $I=1$ ) of the nitrogenous ligand in the fifth coordination site. This indicates that the imidazole residue of the copolymer is coordinated to the fifth coordination site of CoTPP and that its sixth coordination site was vacant for oxygen binding. Also, the imidazole residues are not coordinated to the planar cobaltporphyrin from both sides in the solid state.

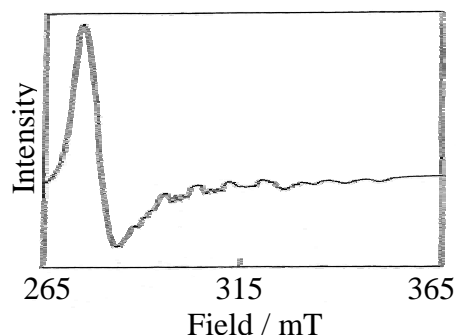


**Figure 3-4.** ESR spectrum of the CoTPP-OIm membrane in an oxygen-free atmosphere at 77K.



The CoTPP-OIm membrane was prepared on a quartz or KBr plate. The CoTPP-OIm membrane displayed a visible absorption spectrum ( $\lambda_{\text{max}} = 528\text{nm}$ ) attributed to CoTPP under a nitrogen atmosphere, which has a good correspondence with that in dichloromethane solution.<sup>12,13</sup> The IR stretching frequency of dioxygen coordinated to the cobalt metal is observed by infrared spectroscopy in a high pressure cell. Coordination of the molecular oxygen in the superoxide type to the Co was confirmed by the observed band at  $1149\text{cm}^{-1}$  (stretching frequency of molecular dioxygen is  $1556\text{cm}^{-1}$ )<sup>14</sup>. These data indicate that the imidazole residue of the copolymer is coordinated to the fifth coordination site of CoTPP and allows reversible and specific oxygen-binding.

### 3.5 CoTPP concentration profile of the CoTPP-OIm membrane

As for the facilitated transport membrane which contains the fixed carrier in the polymer matrix, a homogenous distribution of the carrier molecule is desirable. With the solvent-casting method, for the difference in solubility between the polymer and carrier molecule, the concentration of the carrier will easily be different between the membrane surface and the inside of the membrane, which seriously affects the performance of the facilitated transport through the thin membrane. Therefore, the surface of the CoTPP-OIm thin membrane was analyzed by XPS measurement. The binding energy of the nitrogen, cobalt, and carbon is listed in Table 3-3 and they have good agreement with the reported value<sup>15</sup>. This indicates that the porphyrin exists at the surface of the membrane.

**Table 3-3.** Binding energies for the CoTPP-OIm membrane

Binding energy (eV)	N 1s	Co 2p 3/2	C 1s
Experimental	398.4	779.2	284.7
Reference data <sup>15)</sup>	398.1	779.8	284.1

The composition ratio (Co/C) was calculated from the angle-resolved XPS spectra and plotted vs. the apparent vertical depth (Figure 3-5). The apparent vertical depth of 0 and 1 correspond to the surface and ca 10nm depth from the surface, respectively. The intensity ratio, Co/C, gradually increases with the apparent vertical depth and approaches 1.09; (the elemental feed ratio of cobalt to carbon is ca. 1.09 if the CoTPP-OIm membrane consisted of a homogenous distribution of CoTPP in OIm

matrix). Though the CoTPP quantity is low in most film surface, it can be judged that CoTPP is uniformly distributed in the depth direction.

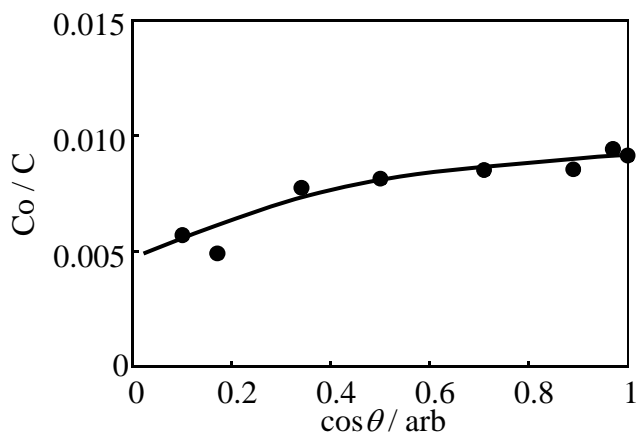


**Figure 3-5.** Depth profile of cobalt atom upon the CoTPP-OIm membrane surface.

By choosing the membrane preparation method and conditions, the carrier (the cobalt porphyrin complex) was uniformly distributed, and it was possible that the property of oxygen facilitated transport also made a thin film of high CoTPP-OIm at less than a 100nm film thickness.

## Reference

1. K. K. Sirkar and W. S. Wo, "Membrane Handbook", Van Nostrand Reinhold, NY (1993).
2. H. Nishide and T. Suzuki, "Handbook of Technology for Separation and Purification", Japan Chemical Society (ed.), Maruzen, Tokyo, (1993), p. 149.
3. L. M Robeson, *J. Memb. Sci.*, **62**, 165 (1991).
4. E. Tsuchida and H. Nishide, *Top. Curr. Chem.*, **132**, 63 (1986).
5. H. Nishide and E. Tsuchida, "Polymers for Gas Separation", N. Toshima ed., VCH publisher, New York, NY (1992), p. 183.
6. H. Nishide, Y. Tsukahara, and E. Tsuchida, *J. Phys. Chem. B*, **102**, 8766 (1998).
7. H. Nishide, H. Kawakami, S. Toda, E. Tsuchida, and Y. Kamiya, *Macromolecules*, **24**, 5851 (1991).
8. J. H. Kim, B. R. Min, J. Won, and Y. S. Kang, *Chem. Eur. J.*, **8**, 650 (2002).
9. J. H. Kim, B. R. Min, C. K. Kim, J. Won, and Y. S. Kang, *Macromolecules*, **35**, 5250 (2002).

10. D. Briggs and M. P. Seah, "Practical Surface Analysis, Vol. 1 Auger and X-ray Photoelectron Spectroscopy", John Wiley & Sons, Chichester, U.K. (1995).
11. C. Ton-That, A. G. Sheard, and R. H. Bradley, *Langmuir*, **16**, 2281 (2000).
12. H. Shinohara, H. Nishide, and E. Tsuchida, *Porphyrins*, **9**, 65 (2000).
13. H. Shinohara, T. Arai, H. Nishide, *Macromol. Symp.*, **186**, 135 (2002).
14. J. O. Alben, "The Porphyrins Vol. III", D. Dolphin ed., Academic Press, New York, NY (1978), pp. 323.
15. D. H. Karweik and N. Winograd, *Inorg. Chem.*, **15**, 2336 (1976).